Proceedings of the 28th IEEE
EMBS Annual International Conference
New York City, USA, Aug 30-Sept 3, 2006

Aortic Thrombus Segmentation using Narrow Band Active Contour Model

Bipul Das, Yogish Mallya, Suryanarayanan Srikanth and Ravikanth Malladi

Abstract— **This paper proposes 2D active contour approach for segmenting thrombus volume from 3D CT images of abdominal aortic aneurysm (AAA). The major challenges in segmenting thrombus are in part because of lack of delineating contrast at anatomical boundaries due to overlap of other soft tissues and artifacts arising from stents and calcium deposits. In the present approach first the bone structures are removed from the image so that these nearby high intensity regions do not interfere in the segmentation process. Next morphological operation is done on the bone-removed image to reduce the effect of streak artifacts. The order of these two operations can be inter-changed. Then, a manual contour is initialized on an axial slice of the pre-processed image and deformed and subsequently propagated to the consecutive slices for deformation. The snake process is governed by force field defined by intensity-based object-ness measure within a band defined by local image properties. The proposed algorithm has been tested on 7 CT images and compared with the ground truth obtained from manual segmentation by radiologist and accuracy between the range 93.16% to 85.08% is observed.**

I. Introduction

Aneurysm is a disease of the aorta that leads to dilation of the lumen structure caused by a progressive weakening of the aortic wall. Aneurysms occur most often in the aorta, the main artery of the chest and abdomen. If not diagnosed and treated, the abdominal aortic aneurysms (AAA) may lead to formation of thrombus which ruptures and blocks of vessels - a leading cause of death. Recent advances in catheter-based technologies have led to exciting new treatments for AAA. This technology requires preoperative planning and a bunch of measurements for proper stent placement. Also, measurements are made for monitoring progress in post-operative follow-up.

Presently, radiologists practice manual delineation of the lumen and the thrombus. This process is time consuming and prone to human subjectivity. An automated method is required that accurately and reproducibly delineates the thrombus with minimal human intervention. The major challenges in segmenting the thrombus structure (the vessel-outer wall) is (a) lack of delineating contrast at anatomical boundaries due to spatially close soft tissues having similar intensities; (b) artifacts due to stents and calcium deposits and (c) undefined geometric structure of the thrombus - which might be symmetric or highly skewed and asymmetric around the lumen.

A number of researches have addressed the issue of thrombus segmentation both in 2D as well as in 3D. Ray propagation techniques [1], [2] propagate radially outward rays from a seed point that are terminated at the vessel-background interface. This technique is quite effective for lumen segmentation in contrast cases, where there is prominent gradient information. However, weak gradients at the outer vessel wall make it inadequate for thrombus segmentation.

Shape and appearance based approaches [3], [4], [5] have been used for delineating the lumen and vessel outer wall. The eigen space derived of the features like intensity and gradient profile of the slices in the training set are used as the *a priori* information into the framework. These methods are quite robust to noise and leakage problems. However, deformability of the shape is restricted by the statistical distribution in the training shapes.

Shiffman *et al.* [6] proposed neural network based multi-level thresholding followed by manual editing for thrombus segmentation. Subasic, *et al.* [7], [8] designed a multilevel level-set based segmentation. In this approach a sphere is initialized inside the aorta and a 2D level-set followed by 3D level-set is done to segment CTA images.

An active contour based **lumen segmentation** is published in [9]. In this approach a number of landmarks are chosen on the vasculature having the diseased vessel and an orthogonal plane is defined. Active contour, which uses gradient information is used for the lumen detection. Finally centerline is detected iteratively from this information.

In this paper we propose a *narrow-band active contour based approach* for segmentation of thrombus from the abdominal aorta. This approach tries to tie in anatomical information, using a narrow-band around a user specified input, to control the deformable framework. The methodology and the flow are discussed in section II. Section III details theory of the proposed narrow-band active contour model. The experimental results and corresponding discussions are done in Section IV and Section V concludes the paper.

II. Methodology

Figure 1 illustrates the various challenging scenarios in the thrombus segmentation. The two major propositions in this paper are (a) the reduction of streak artifacts using a simple morphological closing operation; (b) using objectness and narrow-band approach in deformable contour to effectively segment thrombus. Segmentation is performed on each 2D slice and the result is propagated to next slice and deformed for the entire 3D volume.

Nearby high intensity structures like the bones tend to attract the contour during the process of deformation and it might eventually leak into these structures. To avoid this, initially bone removal is performed on a 3D volume CT data

The authors are affiliated to Imaging Technology, GE Global Research, Bangalore, India - 560066

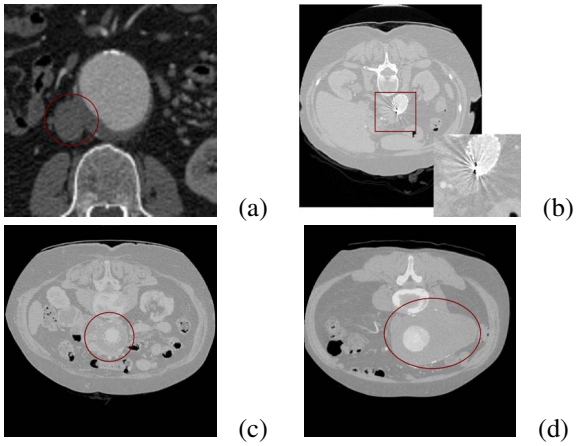

Fig. 1. Different challenges in thrombus segmentation (a) Bridging with soft tissue structure; (b) Streak artifacts; Un-deterministic geometry: (c) symmetric and (d) asymmetric thrombus

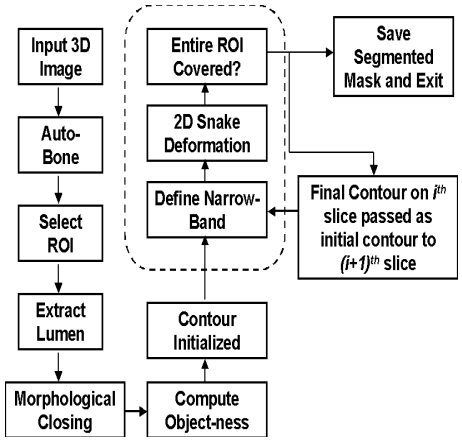

Fig. 2. Thrombus segmentation scheme

using AutoBone^{TM} [10] to get rid of structures like spine and pelvic bones. Lumen having strong intensity feature and well defined gradients also competes with the other rather weak features like the vessel outer wall boundary and often make the contour to snap into it. The lumen is isolated from the artery and an intensity equal to the thrombus mean intensity is used to cover the lumen area.

However, metal and streak artifacts still poses a serious problem is segmenting. Gray-level morphological closing operation of structuring element having a predefined radius is used for this purpose. Fig. 2 illustrates the entire segmentation process and Fig. 3 shows the artifact reduction using morphological operation.

A contour is manually initialized on a preprocessed slice near the thrombus boundary. The deformation of the contour, guided by (a) objectness property defined from *a priori* intensity information, (b) is confined within a narrow band region. Bridging structures often minimizes the delineating contrast at the boundaries. As uncontrolled motion of snake might lead to undesirable result, a narrow band is defined using the local image properties. Final 2D contour in the i^{th} slice is propagated to the next $(i \pm 1)^{th}$ slice and deformed using the similar feature space derived on this slice.

III. Narrow-Band Active Contour

This section develops the active contour theory with the objectness and narrow-band approach.

A. Active Contour: Theory

Active Contour or snake proposed by Kass *et al.* [11] is an energy-minimizing contour that deforms under the action of physics based geometric properties and external constraints defined by image properties, expressed as:

$$E_{snake}(\tau) = E_{int}(\tau) + E_{ext}(\tau) \quad (1)$$

where $E_{snake}(\tau)$ is the total energy of the parametric contour τ, with $\tau \in [0, 1]$. In the discrete domain the contour is defined by an ordered set of points, called control points, upon which all the equations (energy and force) are defined.

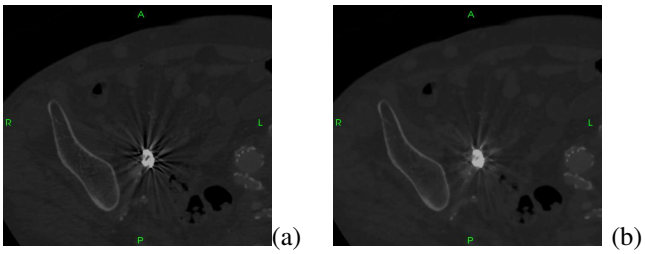

Fig. 3. Streak artifact reduction Image with (a) streak artifact; (b) after morphological operation

$E_{int}(\tau)$ and $E_{ext}(\tau)$ are the internal and external energies [11]. The energy at any point $\vec{v}$ on the contour τ can be expressed as:

$$E_{snake}(\vec{v}) = \alpha\left|\frac{du}{d\tau}\right|^2 + \beta\left|\frac{d^2u}{d\tau^2}\right|^2 - \gamma\left|\nabla I(\vec{v})\right|^2 - \kappa P_{image}(\vec{v}) \quad (2)$$

where the first and second terms of the equation 2 are attributes the geometric properties of the spline with α and β being their controlling factors. The third term is the gradient energy ($\left|\nabla I(\vec{v})\right|^2$) at the location $\vec{v}$ on the image. The fourth term can be constructed from any form of image feature based field at $\vec{v}$.

An image feature needs to be defined such that it has strong directional force in homogeneous regions and weak one near boundaries. Here an intensity based *objectness measure*, attributing this property, is proposed to control the snake deformation. This methodology is in philosophy similar to the approaches in [12], [13], [14]. Let μ_O (μ_B) and σ_O (σ_O) be the mean and standard deviation of the object (background) intensity obtained through prior classification. The intensity distribution is assumed to be one-sided normal distribution, i.e., the value is 1.0 beyond the mean intensity and on the other side it follows a Gaussian distribution [14]. The probabilities, $p_O(f)$ and $p_B(f)$, of any intensity f belonging to object or background respectively can be

defined as:

$$p_O(f) = \frac{1}{\sigma_O\sqrt{2\pi}} e^{\frac{-(f-\mu_O)^2}{2\sigma_O^2}} \quad ; \quad p_B(f) = \frac{1}{\sigma_B\sqrt{2\pi}} e^{\frac{-(f-\mu_B)^2}{2\sigma_B^2}} \tag{3}$$

To define a force field having the following properties: (a) Expanding inside the object; (b) Contracting inside the background; (c) Magnitude should be between $[0, 1]$ and proportional to the confidence level of any pixel's belonging to any region; (d) Weakens when both probabilities are similar, the objectness function is defined as follows:

$$P_{objectness} = p_O - p_B \tag{4}$$

Thus, for pixel having intensity f such that $p_O(f) > p_B(f)$, then $P_{objectness} > 0$ and thus would provide an expanding force directly proportional to $|P_{objectness}|$. In the background region the value of $P_{objectness} < 0$ and the contour point in this region will experience a contracting force field. Near object-background interface the two probabilities becomes similar and $P_{objectness} \rightarrow 0$ and thus weakens itself. In this region the other forces (essentially due to geometric properties) will take the control for deformation.

B. Narrow-band

Radiologists' perceptual sense uses anatomical and physiological knowledge of the growth pattern and shape between slices to delineate the thrombus. For all practical situations, it can be safely assumed that the structural and shape variation of the thrombus is small between two successive slices. To capture the essence of this fact, a narrow-band is defined around the contour and the deformation of each control point is confined within this bound. This band definition can be highly customized depending on the anatomical knowledge. For example, if higher anatomical variation is favored in some direction as opposed to other, then the bandwidth in that direction can be greater. However, in the present application the band has been defined to be of uniform width, since no such directional preference is known in the thrombus case.

The intensity profile along normal to the control points is searched in the pre-defined band. The following situations might be encountered: (a) an object-background interface; (b) calcium deposit giving rise to prominent boundary (a step-up followed by step-down profile) and (c) fuzzy boundary due to bridging. The main intention is to find out true boundary throughout the entire thrombus periphery. A step-down gradient with magnitude above a certain threshold is searched within the band along the normal to the contour points. Prominent gradients are present in situations (a) or (b). The problem arises in regions with condition (c). To restrict leakage through these regions, edges need to be defined based on some criteria. Human perception interpolates missing boundaries using the neighboring information having prominent features. In this approach, a similar philosophy is utilized. For these fuzzy regions, a *pseudo edge* is simulated by interpolation from nearby true gradient information.

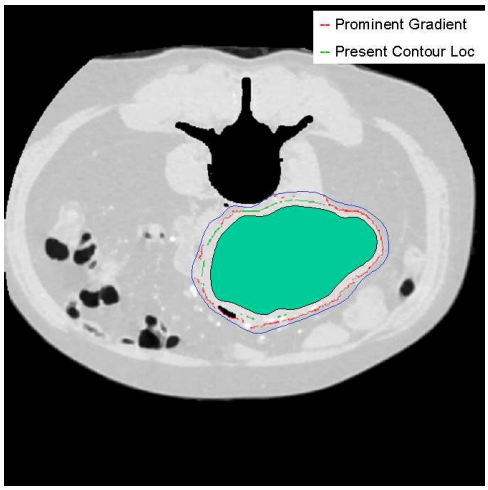

Fig. 4. Illustration of narrow-band - (i) Original search region: between mask boundary and blue line outside; (ii) Prominent Gradient: Red lines; (iii) Initial contour position (no prominent feature observed along the radial lines): green lines

Definition of the narrow band has the following set of assumptions: (a) Contour is initialized near the target boundary; (b) Deformation between two successive slices is small; (c) Anatomical structures other than the one of interest do not have prominent boundaries in the band. While, the first condition is user dependent, the second one is applicable in most cases. But, the third assumption might not be valid in all cases. However, the error introduced is smaller compared to unconstrained contour motion, since in the later case the entire adjacent structure will be selected.

IV. Results and Discussion

The proposed algorithm has been tested on 7 AAA patient CT data sets (in-plane resolution $\approx 0.5mm$ to $0.7mm$ and slice thickness of $0.7mm$ to $1.25mm$) obtained from various sites globally. The cases cover a range of clinically variant situations like (a) contrast cases with and without stents, and (b) non-contrast cases with stent. From the segmentation point of view, the data set includes: (i) morphological variants like (a) symmetric and (b) asymmetric thrombus; (ii) bridging and (iii) artifacts.

The results of these experiments are validated against ground truth from manual segmentation done by two expert radiologists of *Teleradiology Solutions Inc.* at Bangalore, using a similarity metric called Disc Similarity Coefficient (DSC) defined as $DSC = 2\frac{A \bigcap B}{A \bigcup B}$, where A and B are the segmented masks from two methods. The disc similarity coefficient ranged between 93.16% for the best segmentation to 85.08% in the worst case with streak artifacts. The same set of measures were done to find agreement between two radiologists. The results ranged between 94.07% and 90.04%. Figure 5 shows segmented masks overlaid on the original image for some cases.

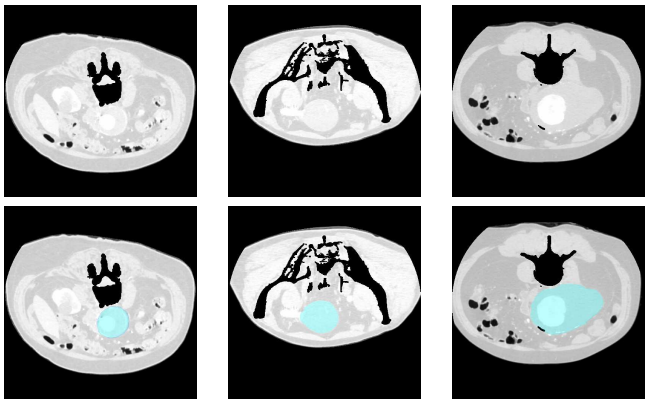

Fig. 5. Segmentation for situations like bridging, streak artifacts, symmetric and asymmetric thrombus. Top row: Original Image Slices; Bottom row: Segmentation result overlaid on the slices

A. Discussion

As previously mentioned, presence of strong feature space in and around the thrombus due to stents and bone challenges the segmentation process. With removal of bone from the image reduced the effect of one of the misleading strong feature. At the same time, it provides with a step-down gradient at the thrombus-bone interface. The stents around the lumen often creates streak artifacts producing false edges into the images. The morphological operation in these regions reduces the effect of these strong features at the stent location. As is seen in Fig. 3, the strong edges reduces considerably. Though a blurring occurs in these regions due to the dilation process, however, the fuzzification helps to get rid of the strong features that would otherwise control the contour motion. The fuzzification of the boundary is dealt separately by introducing the narrow-band approach.

Objectness metric differentiated between object and non-object regions based on pixel property. This function provided a directional property to the snake, thus allowing it to expand or contract based on its location. Unlike the gradient-based uni-directional snake this property prevents leaking into background structures. Also, contour does not latch onto false strong gradients in the non-object region.

The narrow-band approach used nearby strong statistics to fill in for regions with weak features. This prevented uncontrolled snake motion into soft tissues adjacent to the thrombus region without any delineating contrast.

The segmentation results obtained using this active contour model on AAA images show good agreement with manual segmentation by radiologists. The results comparable to the inter-observer variability of manual delineation. Also, a large amount of morphological variation is well captured by the segmentation process. This can be inferred from these results that the proposed properties enables the active contour to delineate the thrombus from other structures.

V. Conclusion

This paper proposed thrombus segmentation from CT images of AAA using active contour. A intensity distribution-based object-ness metric is designed to enrich the snake framework. The introduction of narrow-band captured the structural (anatomical) knowledge and enabled better detection in fuzzy boundary regions, restricting otherwise leakage at those regions. The algorithm has been tested on images with different levels of variance (a) morphological, (b) bridging with other structures, (c) artifacts and (d) clinically varying scenario. The results show high agreement with manual segmentation, used as ground truth.

References

[1] H. Tek, D. Comaniciu, and J. P. Williams, "Vessel Detection by Mean Shift Based Ray Propagation," in *Proc. IEEE WMMBIA*, vol. -, pp. 228–235, 2001.

[2] O. Wink, W. J. Niessen, and M. A. Viergever, "Fast Delineation and Visualization of Vessels in 3-D Angiographic Images," *IEEE Trans. on MI*, vol. 19, pp. 337–346, 2000.

[3] M. de Bruijne, B. van Ginneken, M. Viergever, and W. Niessen, "Adapting Active Shape Models for 3D Segmentation of Tubular Structures in Medical Images," in *Proc. of IPMI*, vol. LNCS - 2732, pp. 136–147, Springer, 2003.

[4] S. D. Olabarriaga, J. M. Rouet, M. Fradkin, M. Breeuwer, and W. J. Niessen, "Segmentation of Thrombus in Abdominal Aortic Aneurysms from CTA with Non-Parametric Statistical Grey Level Appearance Modelling," *IEEE Trans. on MI*, vol. 24, pp. 477–485, 2005.

[5] M. de Bruijne, B. van Ginneken, L. W. Bartels, M. J. van der Laan, J. D. Blankensteijn, W. J. Niessen, and M. A. Viergever, "Automated Segmentation of Abdominal Aortic Aneurysms in Multi-spectral MR Images," in *Proc. of MICCAI; T. Peters and R. Ellis, eds.*, vol. Lecture Notes in Computer Science 2879, pp. 538–545, Springer, 2003.

[6] S. Shiffman, G. D. Rubin, and S. Napel, "Semiautomated Editing of Computed Tomography Sections for Visualization of Vasculature," in *Proc. SPIE Conf. On Medical Imaging*, vol. 2707, pp. 140–151, 1996.

[7] M. Subasic, S. Loncaric, and E. Sorantin, "3D Image Analysis of Abdominal Aortic Aneurysm," in *Proc. SPIE Medical Imaging*.

[8] S. Loncaric, M. Subasic, and E. Sorantin, "3D Deformable Model for Aortic Aneurysm Segmentation from CT Images," in *Proc. of IEEE EMBS*, vol. 22, pp. 398–401, 2000.

[9] K. Subramanyan, S. C. Chandra, and S. K. Pohlman, "Method and Apparatus for Semi-automated Aneurysm Measurement and Stent Planning Using Volume Image Data," *US Patent: US 2004/6782284 B1*, pp. –, 2004.

[10] R. Mullick, R.S. Avila, J.F. Platt, Y. Mallya, R.F. Senzig and J. Knoplioch, "Automatic Bone Removal for Abdomen CTA: A Clinical Review," in *RSNA*, vol. 225, pp. 646 – 646, 2002.

[11] M. Kass, A. Witkin, and D. Terzopoulos, "Snakes: Active Contour Models," *International Journal of Computer Vision*, vol. 1, pp. 321–331, 1988.

[12] J. Ivins and J. Porill, "Statistical Snakes: Active Region Models," in *Proc. of 5th British Machine Vision Conference*, vol. BMVC'94, pp. 377–386, 1994.

[13] B. Das, P. K. Saha, and F. Wehrli, "Object Class Uncertainty Induced Snake with Application to Medical Image Segmentation," in *Proc. SPIE Conf. On Medical Imaging*, vol. 2707, pp. 369–380, 2004.

[14] P. A. Yushkevich, J. Piven, H. Cody, S. Ho, J. C. Gee, and G. Gerig, "User-Guided Level Set Segmentation of Anatomical Structures with ITK-SNAP," *Insight Journal; Sp. Issue, ISC/NA-MIC/MICCAI Workshop on Open-Source Software*, 2005.